Journal of Molecular Liquids 299 (2020) 112241

Contents lists available at ScienceDirect

Journal of Molecular Liquids

journal homepage: www.elsevier.com/locate/molliq

Structure of MF-AlF_3-ZrO_2 (M = K, Na, Li) ionic melts

A.S. Vorob'ev [a], A.V. Suzdaltsev [a,*], P.S. Pershin [a], A.E. Galashev [a,b], Yu.P. Zaikov [a,b]

[a] Institute of High-Temperature Electrochemistry of UB RAS, Yekaterinburg, Russia
[b] Urals Federal University, Yekaterinburg, Russia

ARTICLE INFO

Article history:
Received 7 August 2019
Received in revised form 25 November 2019
Accepted 27 November 2019
Available online 29 November 2019

Keywords:
Structure
Melt
Aluminium
Zirconium
Binding energy
Cation
Complex compounds
Stability

ABSTRACT

Quantum-mechanical calculations by the DFT method and a physical experiment were performed to clarify the type of complexes and their role when using ZrO_2 as a source of zirconium to producing Al-Zr master alloys. The binding energy of complex anions formed from the components Zr-F, Al-O-F and Zr-O-F, whose formation is associated with the dissolution of ZrO_2 and Al_2O_3 oxides in fluoride melts MF-AlF_3 (M = K, Na, Li) was calculated using the program Siesta. The influence of the elemental composition of anions and cation from the second coordination sphere on the binding energy of complex anions is determined. It is shown that filling of the second coordination sphere with Na^+ and K^+ cations shifts the stability from the $[Zr_2O_2F_6]^{2-}$ to $[Zr_2O_2F_7]^{3-}$ complex compound. Replacement of the cation in the second coordination sphere in the row from K to Li leads to lower bond energy in all considered anions. Replacement of aluminium in $[ZrF_x]^{z-}$ and $[Zr_2O_2F_x]^{z-}$ complex groups leads to increasing of ion's size.

The available experimental data on the interaction of ZrO_2 with MF-AlF_3 (M = K, Na, Li) fluoride melts are presented and some new results have been obtained via Raman spectroscopy and XRD.

Based on the comparative analysis of calculations, available and new experimental data concerning interactions in MF-AlF_3-ZrO_2 (M = K, Na, Li) systems it is shown that ZrO_2 dissolution in the MF-AlF_3 melts significantly depends on the radius of the cation of the second coordination sphere. Thus, the ZrO_2 dissolution in the KF-AlF_3 melt takes place with the formation of the K_2ZrF_6 and Al_2O_3 compounds, white in the NaF-AlF_3-ZrO_2 system zirconium complexes and Al_2O_3 appears.

1. Introduction

The fine-grained structure of the produced aluminium is desirable, because determine an improvement of its mechanical properties and performance characteristics due to better homogeneity and reduced porosity. Grinding of aluminium grain is usually carried out by adding metal-grain shredders. In particular, a small addition of zirconium into aluminium (<0.28 wt%) leads to the grinding the grain structure [1,2]. Zirconium can be introduced into molten aluminium via adding of zirconium salts (K_2ZrF_6 or $NaZrF_4$) into the cover salt flux [3,4]. However, the use of such a chemical reagent leads to unpredictable and harmful consequences, such as the release into the atmosphere of gaseous fluoride components (AlF_3, ZrF_4).

More promising methods for production of Al-Zr alloys and master alloys are connected with using of ZrO_2 as a source of zirconium. Also, ZrO_2 is the most available and cheap raw material for producing Al-Zr alloys. In particular, some studies of aluminium-thermic reduction of ZrO_2 are known in systems: CaO-CaF_2 at the temperature of 1600 °C [5], $KClO_3$-S or $NaNO_3$-S at the temperature of 1725 °C [6], NaF-AlF_3 at the temperature of 950–1000 °C [7]. Due to the high yield of zirconium (up to 99.5%), low temperature (750–800 °C) and the possibility of continuous production of Al-Zr master alloys with zirconium content up to 15 wt%, the reduction of ZrO_2 by aluminium under electrolysis conditions in KF-AlF_3-based melts with additives of Al_2O_3 and ZrO_2 oxides is considered to be the most energy efficient [8–10]. However, the reduction kinetics and synthesis parameters largely depend on the composition of zirconium complex compounds formed during the dissolution of ZrO_2 in the oxide-fluoride melt. Earlier we proposed a mechanism of ZrO_2 dissolution in KF-AlF_3-based melts [8], which requires further improvement using other methods.

Similarly, the search for alternative methods of electrolytic production of aluminium leads to need of investigation of the stability of aluminium oxide and oxychloride, as well as the analysis of the role of fluorine anion in the solubility of oxides in chloride melts [11–13]. All these studies suffer from a lack of information about the structures of forming ion complexes.

In this way modelling methods could be a very promising tool for investigation of structural and energy properties, as well as knowledge about vibrations in complex anions. The use the density functional theory (DFT) calculations allow us to directly take into account the exchange and correlation effects. Moreover, using the DFT method, one

* Corresponding author.
E-mail address: suzdaltsev_av@mail.ru (A.V. Suzdaltsev).

https://doi.org/10.1016/j.molliq.2019.112241
0167-7322/

can perform all geometric optimizations without any fixed symmetry. The optimization of the anion geometry showed that the aluminium atom is always five times coordinated, i.e. it is surrounded by four fluorine and one oxygen atoms [13].

To compare the energies of all complexes, we preferably calculate the inherent binding energy. Based on these calculations, the relative stability of the complexes can be compared directly. In [13–15] the complex compounds of aluminium comprehensively reviewed, so there is a possibility to verify the previously obtained data in the present work.

In [15] is shown that the replacement of aluminium with zirconium in fluoride and oxide-fluoride complexes leads to decreasing of binding energy in present complex compounds. The binding energy of the most stable $[Al_2O_2F_4]^{2-}$ complex equals to −158.6 eV, the replacement of aluminium with zirconium leads to decreasing of binding energy to −209.5 eV. It is shown that among $[Zr_2O_2F_x]^{z-}$ complexes, anion $[ZrAlO_2F_6]^{2-}$ have a minimal binding energy. Also, the binding energy in mixed aluminium-zirconium $[ZrAlO_2F_x]^{z-}$ complexes was higher than both $[Al_2O_2F_x]^{z}$ and $[Zr_2O_2F_x]^{z-}$ complexes.

The aim of the present work is study of the stability and geometric structure of zirconium complexes, obtained in the MF-AlF_3-ZrO_2 (M = K, Na, Li) melts using quantum mechanical methods and experimental data.

Recently a significant number of scientific and technical issues about the influence of the complexation factor on the processes of electrolytic production of aluminium have been solved by means of model calculations [16–18]. Therefore, in addition to expanding the concepts of complexation in the fluoride melts with additives of the Al_2O_3 and ZrO_2 oxides, the data obtained in the work can be used for modelling the processes occurring in the melt and on the electrodes in the traditional cryolite-alumina melt with additives (impurities) KF and ZrO_2.

2. Experimental

2.1. Calculation methodology

The most effective approach to the calculation of the binding energy and crystal lattice dynamics proposed in the works of Kohn, Hohenberg and Sham [19,20]. The essence of this method is determined by the following theorem: the energy of the basic state of the system of interacting electrons in the field of atomic nuclei is a unique functional of the electron density distribution $\rho(r)$ (the Kohn-Sham functional). When varying $\rho(r)$, this functional reaches its extreme (minimum), which is equal to the energy of the basic state of the system. The calculations were performed via the hybrid cluster-type computer "URAN" in the Institute of Mathematics and Mechanics of UB RAS. For calculations, the software package SIESTA was used. Performing geometric optimization involved the use of general gradient approximation in the form of Perdew-Burke-Ernzerhof [21], by diagonalization without fixing the coordinates. The dynamic relaxation of atoms continued until the change of the total energy of the system was fewer than 0.001 eV. The cut-off energy of the plane wave basis was 200 Ry. Three parameter exponential basis functions and polarization (TZP) consistent basis sets were used for all calculations. In the present work the influence of the second coordination sphere on the stability of zirconium fluoride, oxide-fluoride complexes and also mixed aluminium-fluoride complex compounds is investigated. The second coordination area was defined as follows: addition of K^+ or Na^+ one cation; addition of K^+ or Na^+ two cations and addition of K^+ one cation and Na^+ one cation.

3. The binding energy was calculated by the equation

$$E_{bond} = E_{compex} - {}^{E_{bond}=E_{compex}-} \sum_{element} n_{element} E_{element} \quad (1)$$

where $E_{complex}$ is total energy of complex, $E_{element}$ is the energy of an isolated anion (F^-, O^{2-}) or cation (Zr^{4+}, Al^{3+}, Na^+, K^+), and $n_{element}$ is number of anions (F^-, O^{2-}) and cations (Zr^{4+}, Al^{3+}, Na^+, K^+) in complex compound.

3.1. ZrO_2 dissolution

Melts for experimental measurements were prepared from individual fluorides (JSC "Vekton", Russia) according to the method described earlier [22,23]. The prepared melt was exposed to purification by potentiostatic electrolysis for 2 h. The concentration of oxygen in prepared melts did not exceed 0.1 wt% in terms of Al_2O_3 according to the oxygen analyzer (LECO Corp, USA). The experiments were carried out in air in a glassy carbon crucible with 200 g of melt at a temperature of 800 °C. Dosed for 30 min 0.5 or 1.0 wt% of ZrO_2 (Chemically pure, JSC "Vekton", Russia) was introduced into the obtained melt while the melt was mechanically stirred. After that the melt was held in isothermal conditions (±4 °C) within 1 h for ZrO_2 complete dissolution [8]. Than the melt samples were taken. Sampling was carried out by freezing of salt on the glassy carbon rod.

3.2. Analysis of the solidified salts

Along with the previously obtained results [8], in present paper Raman spectroscopy methods and XRD where used for analysis the products of ZrO_2 interaction with MF-AlF_3 (M = K, Na, Li) melts. In particular, the interaction products in melts with various [MF]/[AlF_3] molar ratios were studied at the temperature of 800 °C.

The element composition of the melts under study was controlled via spectral analysis using the optical emission spectrometer iCAP 6300 Duo (Thermo scientific, USA). XRD analysis of the solidified products of interaction was carried out using diffractometer D/MAX-2200VL/PC (Rigaku, Japan). Raman spectra were obtained using a Raman microscope-spectrometer U1000 (Renishaw, UK). Lasers with wavelengths of 532 and 633 nm were used as exciting light sources. The microscope can record Raman spectra for objects smaller than 1 μm and has an absolute sensitivity up to 10^{-12} g.

4. Results and discussion

4.1. The binding energy in complexes

Binding energy is equivalent to the energy required to disassemble a whole system into separate parts. A complex system usually has a lower potential energy than the sum of its constituent parts. In other words, with this energy, parts of the system are held together. This often means that energy is released when a bound state is created. The compound is stable if the total potential energy of its parts is negative. It is definition of binding energy (see the Eq. (1)) that we will adhere in this work. Figs. 1 and 2 show all calculated binding energies for zirconium and zirconium-aluminium oxide-fluoride complexes depending on the complex composition and occupancy of the second coordination sphere. From the presented data it follows that the minimal binding energy has $[Zr_2O_2F_7]^{3-}$ complex. The relationship between the adsorption energy and the type of ions filling the second coordination sphere is found. Thus, the replacement of potassium atoms with sodium atoms in the second coordination sphere leads to a decrease in the binding energy from 1 to 3% depending on the composition of the complex compound. The geometric structure of this complex is shown in Fig. 3. Figure of complex structures were made by Avogadro program.

4.2. The binding energy in $[ZrF_y]^{z-}$ complexes

Fig. 1 shows the dependence of the binding energy of zirconium complexes on the number of potassium and sodium cations. The $[ZrF_6]^{2-}$ complex has the lowest binding energy in all considered cases. The addition of Na^+ and/or K^+ cations to the second coordination sphere leads to a decrease in the binding energy of the complex and

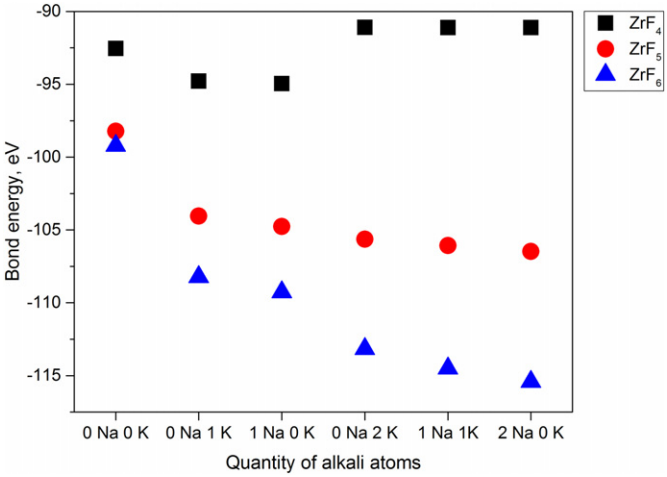

Fig. 1. Dependence of the binding energy of zirconium fluoride complexes on the quantity of potassium and sodium cations in the second coordination sphere.

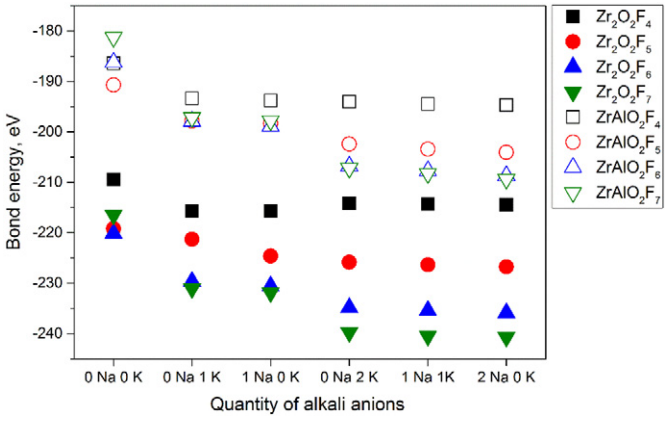

Fig. 2. Dependence of the binding energy of zirconium and mixed aluminium-zirconium oxide-fluoride complexes on the quantity of potassium and sodium cations in the second coordination sphere.

therefore to an increase of its stability. When two ions are neighbors of the second order, complexes containing sodium in the second coordination sphere has a 1–2% lower binding energy than those containing the same amount of potassium cations. The geometric structure of the $[ZrF_6]^{2-}$ complex with the addition of two Na^+ cations is shown in Fig. 4.

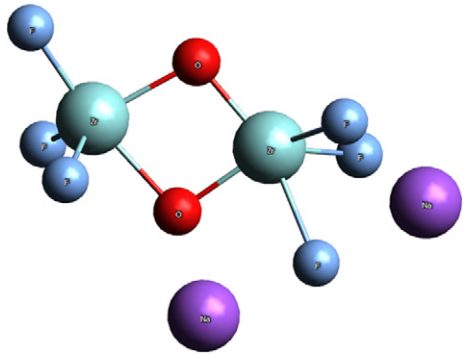

Fig. 3. Geometry of the $[Zr_2O_2F_7]^{3-}$ complex with two Na^+ cations in the second coordination sphere.

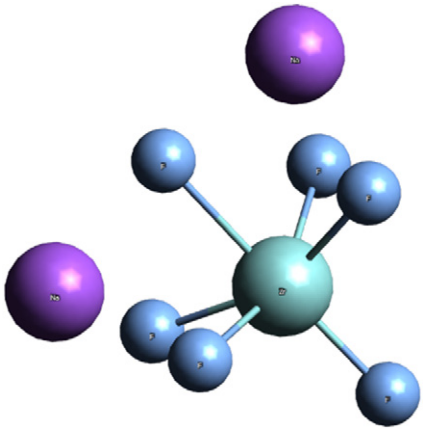

Fig. 4. Geometry of the $[ZrF_6]^{2-}$ complex with two Na^+ cations in the second coordination sphere.

4.3. The binding energy in $[Zr_2O_2F_y]^{z-}$ and $[ZrAlO_2F_y]^{z-}$ complexes

Fig. 2 shows the dependence of the binding energy of both zirconium oxide-fluoride and the corresponding mixed zirconium-aluminium complexes on the number of potassium and sodium cations in the second coordination sphere. As can be seen, the $[Zr_2O_2F_6]^{2-}$ ion has the lowest binding energy (−220.14 eV) in the absence of alkali metal cations. When potassium and/or sodium cations are added, the most stable becomes $[Zr_2O_2F_7]^{3-}$ complex. Addition of cations to the second coordination sphere of the $[Zr_2O_2F_7]^{3-}$ complex leads to a decrease of the compound binding energy, consequently an increase of its stability.

The binding energy of mixed aluminium-zirconium oxide-fluoride complexes is 10–15% less than zirconium oxide-fluoride complexes. The $[ZrAlO_2F_5]^{2-}$ complex has the lowest binding energy (−190.69 eV) in the mixed aluminium-zirconium complex group in the absence of alkali metal cations. When one potassium or sodium cation is added, the most stable are $[ZrAlO_2F_5]^{2-}$, $[ZrAlO_2F_6]^{3-}$, $[ZrAlO_2F_7]^{4-}$ complexes with a binding energy difference <1 eV. At the same time, a $[ZrAlO_2F_6]^{3-}$ complex has the lowest binding energy (−198.90 eV). The addition of two cations to the second coordination sphere leads to a decrease in the binding energy. The binding energy of $[ZrAlO_2F_5]^{2-}$ complex becomes ≈5 eV higher than binding energies of $[ZrAlO_2F_6]^{3-}$ and $[ZrAlO_2F_7]^{4-}$ complexes. Geometric structure of the most stable $[ZrAlO_2F_7]^{4-}$ complex with two sodium cations are added to the second coordination sphere is shown in Fig. 5.

4.4. Geometry of the complexes

Calculations show that the introduction of potassium and/or sodium cations into the second coordination sphere of complexes changes the

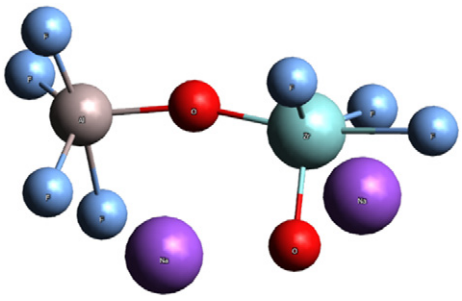

Fig. 5. Geometry of the $[ZrAlO_2F_7]^{4-}$ complex with two Na^+ cations in the second coordination sphere.

Zr—F and Zr—O bond lengths within 2–4%. Table 1 shows the values of the average bond lengths in complexes of zirconium and aluminium. Thus, the Me-F bond lengths increase with increasing fluorine content in the compound. At the same time, the length of the Al—F bond in all the considered compounds are less than the Zr—F bonds by 8–12%. The data about the value of the Al—F bond lengths are 1–3% upward than those values obtained in [24]. The Zr—O bond lengths in zirconium oxide-fluoride complexes have the similar values to Zr—F bond lengths and 8–11% more Al—O bond lengths. The lengths of Al—O bonds in these complexes grows from 1.87 to 2.09 A.

From the comparison of bond lengths for fluoride and oxide-fluoride complexes, it can be concluded that when ZrO_2 is added to the fluoride melts, the size of the formed complexes increased.

It is interesting to compare the geometric structure of the zirconium complex on the example of the $[Zr_2O_2F_7]^{3-}$ ion (Fig. 3) and the mixed aluminium-zirconium complex on the example of the $[ZrAlO_2F_7]^{4-}$ ion (Fig. 5). It can be noted that two Zr-O-Zr bridging bonds are formed in zirconium complexes. While in a mixed grouping, a single Zr-O-Al bridging bond and Zr—O bond are formed.

4.5. Analysis of the experimental data

Because the model calculations do not take into account the real interaction of atoms and molecules in bulk of the melt, the experimental data of the composition and structure of the studied systems are summarized in a Table 2 as well as on Figs. 6 and 7.

Comparing the known data, it can be assumed that ZrO_2 dissolution mechanism in MF-AlF_3 (where M = K, Na, Li) melts significantly depends on the radius of the cation in the second coordination sphere. Thus, aluminium- and zirconium-containing oxide complexes (in form of Al_2O_3 and ZrO_2) are found in systems containing NaF [7,27]. However an additional product of ZrO_2 interaction with KF-AlF_3-based melts is K_2ZrF_6.

Figs. 6 and 7 show diffractograms and Raman spectra of frozen MF-AlF_3-ZrO_2 (M = K, Na, Li) samples, confirming previously obtained data. It should be noted that the KF-AlF3-ZrO_2 system is characterized by the appearance of K_2ZrF_6 in the interaction products, the NaF-AlF_3-ZrO_2 system by the maximum intensity of ZrO_2 peaks, and the LiF-AlF_3-ZrO_2 system by the maximum peak intensity of fluoroaluminate complexes. All this indicates the difference in the ways of ZrO_2 dissolution in the studied melts.

Based on the model calculations and experimental data we can conclude that ZrO_2 interaction with the MF-AlF_3 (M = K, Na, Li) melt may occur with the formation of Al-O-F and Zr-O-F complexes, for example, according the following scheme:

Total reaction: $3ZrO_2 + 6MF + 12MAlF_4 = 3M_2ZrF_6 + 6M_2Al_2OF_6$ (3)

Step 1: $3ZrO_2 + 2MF + 4MAlF_4 = 3M_2ZrF_6 + 2Al_2O_3$ (3′)

Step 2: $2Al_2O_3 + 4MF + 8MAlF_4 = 6M_2Al_2OF_6$ (3″)

Total reaction: $2ZrO_2 + 6MF = M_2Zr_2O_2F_6 + 2M_2O$ (4)

Step 1: $ZrO_2 + 4MF = ZrF_4 + 2M_2O$ (4′)

Step 2: $ZrO_2 + ZrF_4 + 2MF = M_2Zr_2O_2F_6$ (4″)

Total reaction: $2ZrO_2 + 2MF + MAlF_4 = M_2Zr_2O_2F_6 + MAlO_2$ (5)

Step 1: $ZrO_2 + MAlF_4 = ZrF_4 + MAlO_2$ (5′)

Step 2: $ZrO_2 + ZrF_4 + 2MF = M_2Zr_2O_2F_6$ (5″)

Depending on the cation composition, the stability of the zirconates and the capacity of the melts with dissolved oxides, the schemes suggest intermediate stages of Al_2O_3 or ZrF_4 formation. Limiting are the stages of dissolution of Al_2O_3 and ZrO_2 oxides by reactions (3″), (4″) and (5″). It is known that KF-AlF_3 system is characterized by the highest solubility of Al_2O_3 at the same other conditions [14,22,30], and K_2ZrF_6 has a highest solubility in the LiF-NaF-KF systems according to experimental [28,29] and calculated data [15]. This promotes ZrO_2 dissolution in KF-AlF_3 melt by (3)–(5) schemes. The (4) and (5) schemes are more typical for LiF-AlF_3-ZrO_2 and NaF-AlF_3-ZrO_2 systems.

Table 1
Bond lengths in zirconium and aluminium complexes, where Y – Zr or Al, and *x* – number of fluorine ions in a complex compound.

	x	Al-F, Å	Zr-F, Å	Al-O, Å	Zr-O, Å
$[YF_x]$	4	1.76	1.98	–	–
	5	1.83	2.00	–	–
	6	1.90	2.05	–	–
$[Y_2O_2F_x]$	4	1.80	1.99	1.82	2.04
	5	1.84	1.99	1.86	2.03
	6	1.91	2.04	1.87	2.02
	7	–	2.09	–	2.02
$[ZrAlO_2F_x]$	4	1.75	1.97	1.87	2.05
	5	1.74	2.04	1.74	1.92
	6	1.82	2.11	1.95	1.98
	7	1.89	2.17	2.09	1.94

Table 2
Data on interaction between ZrO_2 and molten fluoride systems.

Initial molar composition	ZrO_2 solubility	*T*, °C	Phase composition	Methods	Ref.
1.3KF-AlF_3 + 1 mol% ZrO_2	1.30 mol% at 750 °C	500–800	$KAlF_4$, Al_2O_3, K_2ZrF_6, ZrO_2, gaseous Zr-containing compounds was not detected	XRD, DSC, TG, ICP	[8]
1.5KF-AlF_3 + 1 mol% ZrO_2	1.25 mol% at 750 °C				
1.1KF-0.2NaF-AlF_3 + 1 mol % ZrO_2	1.28 mol% at 750 °C		$KAlF_4$, $K_2NaAl_3F_{12}$, Al_2O_3, K_2ZrF_6, ZrO_2		
2.4NaF-AlF_3 + 1 wt% ZrO_2	>3 wt% at 1000 °C	1000	Na_3AlF_6, ZrO_2	XRD	[7]
AF-ZrF_4 (A = Li, Na, K)			The predominance of the ZrF_6^{2-} ion is noted, while its stability strongly depends on the cation and is maximal in the case of potassium	Spectroscopy, molecular dynamics simulations	[25]
AF-ZrF_4 (A = Li, K, Cs)		Up to 1000	ZrF_6^{2-}, ZrF_7^{3-}	Raman spectroscopy	[26]
FLiNaK + ZrO_2 FLiNaK + ZrF_4 + ZrO_2	0.02 mol kg^{-1}	600	$Zr_2OF_x^{6-x}$	LECO oxide analyzer, Raman spectroscopy	[27]
1.3LiF-AlF_3 + 1 mol% ZrO_2	1.12 mol% at 800 °C	800	Li_3AlF_6, AlF_3, Al_2O_3, ZrO_2	XRD, ICP, Raman spectroscopy	Present work
1.3NaF-AlF_3 + 1 mol% ZrO_2	1.27 mol% at 800 °C		$NaAlF_4$, Na_3AlF_6, $Na_5Al_3F_{14}$, ZrO_2		
1.3KF-AlF_3 + 1 mol% ZrO_2	1.47 mol% at 800 °C		$KAlF_4$, Al_2O_3, K_2ZrF_6, ZrO_2		

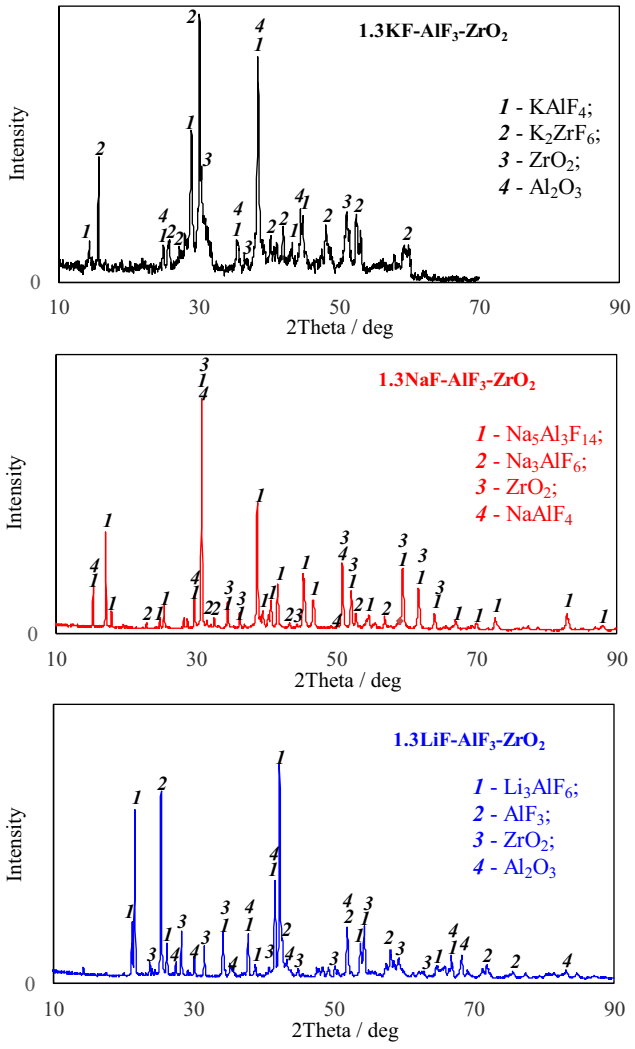

Fig. 6. X-Ray diffraction analysis data of frozen melts MF-AlF_3-ZrO_2.

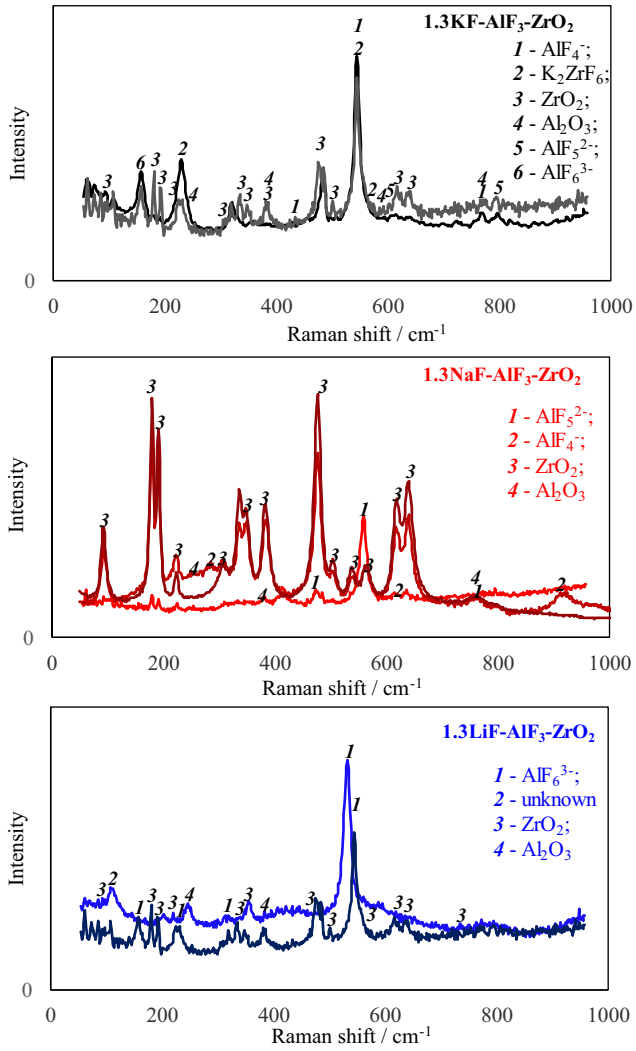

Fig. 7. Raman spectra for frozen melts MF-AlF_3-ZrO_2.

5. Conclusion

Structure of the MF-AlF_3-ZrO_2 (M = K, Na, Li) ionic melts was studied by means of theoretical calculations and physical analysis methods.

As a result of calculations, it was shown that among complexes of the Zr—F composition, the $[ZrF_6]^{2-}$ complex has the lowest binding energy regardless of the composition of the second coordination sphere. With the introduction of oxygen atoms, the binding energies in the complexes formed decrease approximately halved. Depending on the radius of the cations in the second coordination sphere, the complexes $[Zr_2O_2F_6]^{2-}$ and $[Zr_2O_2F_7]^{3-}$ possess the lowest binding energy.

Addition of Na^+ or K^+ cations to the second coordination sphere of the $[ZrF_x]^{z-}$, $[Zr_2O_2F_x]^{z-}$, and $[ZrAlO_2F_x]^{z-}$ complex groupings changes the bond lengths of Zr—F and Zr—O in the range of 2–4% and leads to an increase in the stability of these compounds in the melt. Moreover, the replacement of K^+ with Na^+ cations in the second coordination sphere is the reason for the decrease in the binding energy by 1–3% depending on the complex compound.

Based on the calculated results, geometric structures of the most typical Zr-O-F complexes are constructed. Shown, that the addition of ZrO_2 into the MF-AlF_3 (M = K, Na) melts leads to an increase in the geometric dimensions of the resulting complex compounds in the melt and provokes a decrease in diffusion.

New experimental results were obtained regarding the phase composition of the MF-AlF_3-ZrO_2 systems, based on which probable dissolution schemes of ZrO_2 dissolution in the melts under study are suggested.

CRediT authorship contribution statement

A.S. Vorob'ev: Formal analysis, Resources, Visualization, Writing - original draft. **A.V. Suzdaltsev:** Conceptualization, Supervision, Writing - original draft. **P.S. Pershin:** Resources, Writing - original draft. **A.E. Galashev:** Supervision, Writing - review & editing. **Yu.P. Zaikov:** Funding acquisition, Supervision.

Declaration of competing interest

The authors declare that they have no known competing financial interests or personal relationships that could have appeared to influence the work reported in this paper.

Acknowledgments

The DFT calculations were performed via the hybrid cluster-type computer “URAN” in the Institute of Mathematics and Mechanics of UB RAS and the facilities of the shared access center “Composition of Compounds” of Institute of High-Temperature Electrochemistry UB RAS were used in this work.

References

[1] K. Knipling, D. Seidman, D. Dunand, Acta Mater. 59 (2011) 943–954.
[2] A. Kataev, O. Tkacheva, I. Zakiryanova, A. Apisarov, A. Dedyukhin, Y. Zaikov, J. Mol. Liquids 231 (2017) 149–153.
[3] A. Suzdaltsev, A. Filatov, A. Nikolaev, A. Pankratov, N. Molchanova, Y. Zaikov, Russian Metallurgy (Metally) (2018) 133–138.
[4] A. Azarniya, A. Taheri, K. Taheri, J. Alloys & Comp. 781 (2019) 945–983.
[5] S. Agafonov, S. Krasikov, A. Ponomarenko, L. Ovchinnikova, Inorg. Mater. 48 (2017) 813–820.
[6] J. Juneja, Indian J. of Eng. & Mater. Sci 9 (2002) 187–190.
[7] M. Li, Y. Li, Z. Wang, J. Electrochem. Soc. 166 (2) (2019) D65–D68.
[8] P. Pershin, A. Kataev, A. Filatov, A. Suzdaltsev, Y. Zaikov, Metall. & Mater. Trans. B 48 (2017) 1962–1969.
[9] A. Filatov, P. Pershin, A. Nikolaev, A. Suzdaltsev, Tsvetnye Metally 11 (2017) 27–31.
[10] A. Filatov, P. Pershin, A. Suzdaltsev, A. Nikolaev, Y. Zaikov, J. Electrochem. Soc. 165 (2) (2018) E28–E34.
[11] G. Picard, F. Seon, B. Tremillon, J. Electroanal. Chem. and Interfacial Electrochem. 102 (1) (1979) 65–75.
[12] G. Picard, F. Seon, B. Tremillon, Y. Bertaud, Electrochim. Acta 25 (1980) 1453–1462.
[13] G. Picard, F. Bouyer, M. Leroy, Y. Bertaud, S. Bouvet, J. Mol. Structure 368 (1996) 67–80.
[14] E. Robert, J. Olsen, V. Danek, E. Tixhon, T. Ostvold, B. Gilbert, J. Phys. Chem. B 101 (1997) 9447–9456.
[15] A. Vorob'ev, A. Suzdaltsev, A. Galashev, Russian Metallurgy (Metally) (2019) 781–786.
[16] J. Hvonbarner, K. Andersen, R. Berg, J. Mol. Liquids 83 (1999) 141–151.
[17] M. Chrenkova, V. Danek, R. Vasiliev, A. Silny, V. Kremenetsky, E. Polyakov, J. Mol. Liquids 102 (2003) 226–231.
[18] A. Galashev, O. Rakhmanova, Modelling & Simulation in Mat. Sci. and Eng. 26 (2017), 025003.
[19] P. Hohenberg, W. Kohn, Phys. Review B 136 (1964) 864–871.
[20] W. Kohn, L. Sham, Phys. Review A. 140 (1965) 1133–1138.
[21] J. Perdew, K. Burke, M. Ernzerhof, Phys. Review Letters 77 (1996) 3865–3868.
[22] A. Apisarov, A. Dedyukhin, A. Redkin, O. Tkacheva, Y. Zaikov, Rus. J. Electrochem. 46 (2010) 633–639.
[23] A. Nikolaev, A. Suzdaltsev, Yu. Zaikov, J. Electrochem. Soc. 166 (8) (2019) D252–D257.
[24] X. Lv, Z. Han, C. Guan, L. Jiang, S. Wu, Phys. Chem. Chem. Phys. 21 (2019) 16573–16582.
[25] O. Pauvert, M. Salanne, D. Zanghi, Ch. Simon, S. Reguer, D. Thiaudiere, Y. Okamoto, H. Matsuura, C. Bessada, J. Phys. Chem. B 115 (2011) 9160–9167.
[26] V. Dracopoulos, J. Vagelatos, G.N. Papatheodorou, J. Chem. Soc. Dalton Trans. (2001) 1117–1122.
[27] M. Shen, H. Peng, M. Ge, C. Wang, Y. Zuo, L. Xie, RSC Adv. 5 (2015) 40708–40713.
[28] B. Kubıkova, I. Mackova, M. Boca, Monatsh Chem 144 (2013) 295–300.
[29] V. Pavlik, P. Barborik, M. Boca, Z. Vaskova, Chem. Pap. 70 (2) (2016) 197–205.
[30] V. Danielik, J. Hives, J. Chem. Eng. Data 49 (2004) 1414–1417.